catalysts

MDPI

Article

# Passive Solar Photocatalytic Treatment of Emerging Contaminants in Water: A Field Study

**Gisoo Heydari [1,*], Cooper H. Langford [2] and Gopal Achari [1]**

[1] Department of Civil Engineering, University of Calgary, 2500 University Dr. NW, Calgary, AB T2N 1N4, Canada; gachari@ucalgary.ca

[2] Department of Chemistry, University of Calgary, 2500 University Dr. NW, Calgary, AB T2N 1N4, Canada; chlangfo@ucalgary.ca

* Correspondence: gisoo.heydari@ucalgary.ca

Received: 3 November 2019; Accepted: 5 December 2019; Published: 9 December 2019


**Abstract:** Global economic shifts towards utilization of solar energy provides opportunities for photocatalytic technologies that can harness this abundant source of energy for treatment of organic contaminants. The majority of studies in this area have been performed under artificial light, whereas in this paper, the efficacy of passive photocatalysis was studied under sunlight. Buoyant titanium dioxide ($TiO_2$) coated glass spheres were used to treat 2, 4-dichlorophenoxy acetic acid (2, 4-D), methyl chlorophenoxy propionic acid (MCPP), and 3, 6-Dichloro-2-methoxy benzoic acid (Dicamba) in Killex®, a commercially available herbicide. Furthermore, photocatalytic degradation of sulfolane and a typical naphthenic acid (cyclopentane carboxylic acid—CPA) were also tested under ambient conditions. The results showed 99.8% degradation of 2, 4-D, 100% degradation of both MCPP and Dicamba in Killex® solution, and 97.4% degradation of sulfolane by capturing 3.18 MJ/m$^2$ solar energy. Total organic carbon (TOC) was decreased by 88% and 64% in both solutions, respectively. TOC of the aqueous solution containing 20 ppm CPA was also decreased by 78.4% with 7.8 MJ/m$^2$ energy. Despite the slow kinetics and the temporal variations of sunlight in northern latitudes, the results indicated that passive photocatalysis is a promising approach for treatment of contaminants under ambient conditions.

**Keywords:** passive treatment; solar; photocatalysis; herbicide; naphthenic acids; sulfolane

## 1. Introduction

The installation of solar driven technologies has grown significantly over the last decade; however, there is still a significant gap between the potential and actual application of sunlight for water treatment [1–3]. When solar energy is captured and used directly, the treatment process does not require additional sources of power [4]; hence it is referred to as a "passive system" [1,5]. The shift towards use of solar energy for water treatment reduces the carbon footprint of the process [6]. It also becomes economically attractive, especially for remote locations where there is limited access to power grids [7,8].

The main solar driven processes for water treatment are solar powered desalination plants (in the megawatt range), smaller solar thermal desalination plants (in the kilowatt range), and disinfection and detoxification systems. The latter uses near ultraviolet (UV) and visible light spectrums for solar photocatalysis through the generation of highly reactive oxidizing species that break the organic contaminants and destroy the pathogenic organisms [7,9]. Heterogeneous photocatalysis using titanium dioxide ($TiO_2$) and many other photocatalysts has been used for water disinfection, treating industrial wastewaters, as well as waters contaminated with non-point source pollutants such as pesticides [10–15].

Titanium dioxide is the most common and inexpensive photocatalyst. It is non-toxic, photo-stable, and chemically inert and mechanically robust [16–19]. Near UV photons with wavelengths shorter than 386 nm that can produce energy greater than the oxidation potential of $TiO_2$ (3.02 V for rutile phase and 3.2 V anatase phase), are required to excite an electron from its valence band to conduction band, initiating the photocatalytic degradation reactions [13]. Only a small fraction (3%–5%) of sunlight irradiation reaching earth can produce the required energy to achieve this band-gap excitation [20,21].

$TiO_2$ is used in various physical forms such as powder or on engineered substrates where nanostructures are grown [16,22]. The main challenge associated with using the powder form is the separation of fine particles from the solution after treatment. Hence, it is preferred that $TiO_2$ nano-particles be supported on a media such as glass, alumina, silica, and ceramic [23–28].

The majority of heterogeneous photocatalytic systems use the photocatalyst in a slurry or supported form inside concentrating and non-concentrating reactors to treat contaminants in water [7,18,29–32]. Falling film and shallow solar ponds are non-concentrating reactors [33]. In the falling film system, the liquid falls slowly over a photocatalyst that is supported on the surface of a tilted plate that faces the sun and is open to the atmosphere [34]. Falling film systems with coated $TiO_2$ have been studied for degradation of phenol and achieved 99.3% removal [35]. In the shallow solar pond system, the catalyst can be used in a slurry form or as a fixed bed. In the slurry form, fine catalyst particles are dispersed throughout the pond and require repetitive agitation. In the fixed bed, the catalyst is supported, which allows a higher throughput but results in a lower degradation efficiency [32,34,36]. Non-concentrating reactors are advantageous because of their simple design and usage of both direct and diffuse parts of UV light. Consequently, a higher quantum efficiency can be achieved but a much larger reactor area is required. Moreover, the supporting media of the photocatalyst may scatter the light, preventing its penetration and acting like a screen, thereby decreasing its effectiveness. To avoid these effects, a floating support is preferred [25,26,28].

In a 1991 patent, Brock and Heller explained the application of $TiO_2$ coated floating beads for oxidation of organic compounds in water [37]. The invention was a turning point for application of the passive photocatalytic systems for contaminated water treatment. The floating beads were to be used, under sunlight, for oil spills on water. The 10–30 μm beads were made of plastic (polyethylene or polypropylene) covered with a layer of silicon dioxide or aluminum oxide, which prevented photocatalysis of the organic bead material [37]. Since then, $TiO_2$ supported on floating beads and its composites have been synthesized [38–40] and tested in conventional reactors and under sunlight on a wide range of contaminants, including organo-phosphorus pesticides [41], nitrite [42], formic acid [40], and industrial dyes [39].

Currently, there are very few studies on passive photocatalysis outside of conventional reactors for the treatment of contaminated waters under sunlight [9,43–45]. The majority of passive applications are reported for purification of air [16], self-cleaning construction materials such as ceramics and tiles [4,46], and for the destruction of airborne volatile organic contaminants in high traffic areas [47].

Passive solar driven photocatalysis has been investigated for treatment of agricultural wastewater using $TiO_2$ nanoparticles coated on porous ceramic plates [48], degradation of different dyes using $TiO_2$ (P25) covered on polystyrene and high density polyethylene beads [49,50], and treatment of tetracycline from agricultural wastewater using $TiO_2$ deposited within a porous polymeric film on the surface of the floating acrylic spheres [43]. Floating photocatalysts based on salicylic acid (SA)-modified $TiO_2$ immobilized on small pieces of palm wood, as buoyant support, were also studied for degradation of Congo red [51]. $TiO_2$ covered on buoyant hollow glass microspheres was used for treatment of groundwater contaminated with aromatic amino-compounds. The concentration of xylidine decreased from 280 mg/L to less than 25 mg/L over a 36 day period of insolation [45]. A similar photocatalyst was also investigated for degradation of naphthenic acids in oil sands process affected water [52]. Although more than 80% degradation efficiency was achieved, it was lower in comparison to $TiO_2$ powder that achieved 98% degradation of acid-extractable organics. Degradation of humic substances in the presence of $TiO_2$ coated glass spheres was studied under 365-nm low-pressure mercury lamps.

The results showed that the performance of the photocatalyst coated glass spheres was lower compared to the slurried $TiO_2$ [25]. Although supported photocatalysts had lower efficiency, they had certain advantages in the passive systems in terms of energy consumption and feasibility for environmental applications [53]. However, higher photocatalytic performance can be achieved using crystal growth technologies that produce {001} and {110} crystal facets with higher photocatalytic activity [54–57], and generate structures with higher surface area such as multi-shell $TiO_2$ [58,59], and flower-like $TiO_2$ on nano-sheets [60], which is beyond the scope of this research.

The main driver of this research was to test a treatment option that can be used in remote regions in northern climates. In such regions, there are limited commercially viable treatment options available, and in many cases no access to the power grid. To achieve this objective, a variety of the common emerging contaminants of concern were selected and the efficacy of a passive solar driven photocatalysis under sunlight was investigated. To date, there is no field study on passive solar photocatalysts of the selected contaminants in the northern climate.

Cyclopentane carboxylic acid (CPA), Killex®, and sulfolane were three emerging contaminants studied here. CPA is the simplest naphthenic acid that is found in oil sand process affected water (OSPW). OSPW is produced during oil sand surface mining processes in Alberta, Canada. Approximately 80% of this waste water is recycled and reused [61]. The remaining is stored in tailings ponds due to the zero discharge policy in Alberta that prohibits the release of industrial wastewater in the environment [62]. Tailings ponds are located in remote locations. Although there is extensive research ongoing in this area [63–65], there is currently no commercial treatment methodology available for the water stored in the tailings ponds.

Killex® is a selective and commercially available herbicide that contains 2, 4-dichlorophenoxy acetic acid (2, 4-D), methyl chlorophenoxy propionic acid (MCPP or Mecoprop-P), and 3, 6-dichloro-2-methoxybenzoic acid (Dicamba). Killex® constituents are present in surface and ground waters as a result of herbicide usage in lawns and agricultural lands [66]. The chemical 2, 4-D is one of the best-studied phenoxy herbicides [67]. It has a low biodegradability with potential health effects; therefore, it is categorized as an emerging environmental contaminant [68,69]. Due to its high mobility, runoff from agricultural lands to non-targeted areas and water bodies is common [66]. A pesticide baseline study on the semi-permanent wetlands of the Aspen region in Alberta, Canada showed that 2, 4-D is amongst the most frequent contaminants in water and precipitation samples [70]. The passive photocatalytic system has also been tested on sulfolane. Sulfolane is a water-miscible industrial solvent used in gas processing plants [71,72]. It has entered aquifers and groundwater through landfills and unlined storage ponds and spills [73]. A significant groundwater contamination by sulfolane was reported in Alaska [74] The molecular structures of the studied contaminants are illustrated in Figure 1.

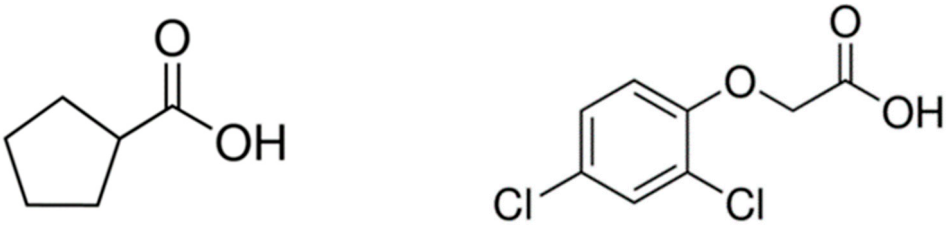


(**a**) (**b**)

**Figure 1.** *Cont.*

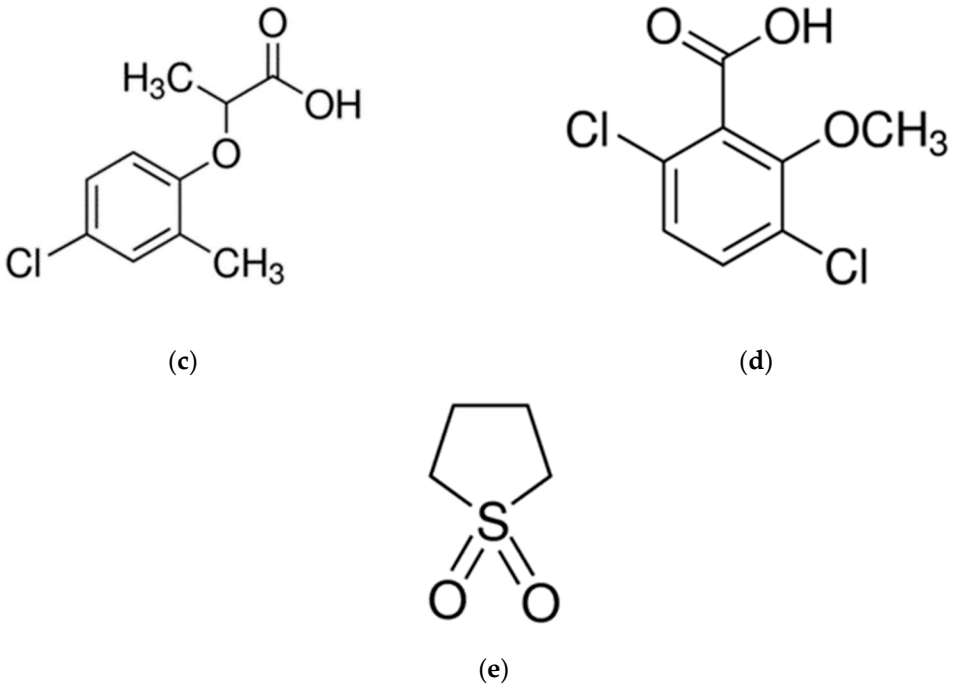


**Figure 1.** Chemical structures of the studied contaminants: (**a**) CPA, (**b**) 2, 4-D, (**c**) MCPP, (**d**) Dicamba, (**e**) Sulfolane.

$TiO_2$ coated glass spheres were chosen as typical photocatalysts to investigate the effectiveness of solar energy to initiate photocatalytic reactions in the ambient environment. Studies were conducted in the field, at the University of Calgary's Weather Research Station (latitude: 51°, 4′ N, and longitude: 114°, 8′ W; altitude: 1114 m), which enabled access to real-time solar irradiation data. Experiments were conducted from August to November 2016.

## 2. Results and Discussion

### *2.1. CPA*

The concentration of CPA was reduced by 47% and 69% after 4 h of irradiation at catalyst loadings of 1.13 mg/cm$^2$ and 3.96 mg/cm$^2$, respectively; 5.9 MJ/m$^2$ energy was received from sunlight, and considering the assumptions stated in Section 5.3, 0.14 MJ/m$^2$ of it was captured by photospheres from UV light. CPA was not detectable after two days of insolation at the catalyst loading of 3.96 mg/cm$^2$ with 1.01 MJ/m$^2$ solar energy. Concentration change in the control samples was negligible.

Samples were insolated for 25 days in order to investigate mineralization of total organic carbon. Figure 2 shows TOC of all samples before and after irradiation. The TOC of the samples with photospheres was reduced by 77% at both catalyst loadings, and the concentration of CPA reached non-detectable levels.

The calculated total energy received during the 25 days of insolation was 325.08 MJ/m$^2$. This amount of energy is equivalent to 7.8 MJ/m$^2$ energy from UV light, which was captured by photocatalyst during insolation. The maximum temperature during daytime was 27.3 °C. The lowest recorded temperature was 1 °C. No freezing temperature or frosting of the samples were observed over the course of experiments. It can be concluded that the photocatalyst is the cause of the photoreaction under direct sunlight as no degradation was observed in the dark.

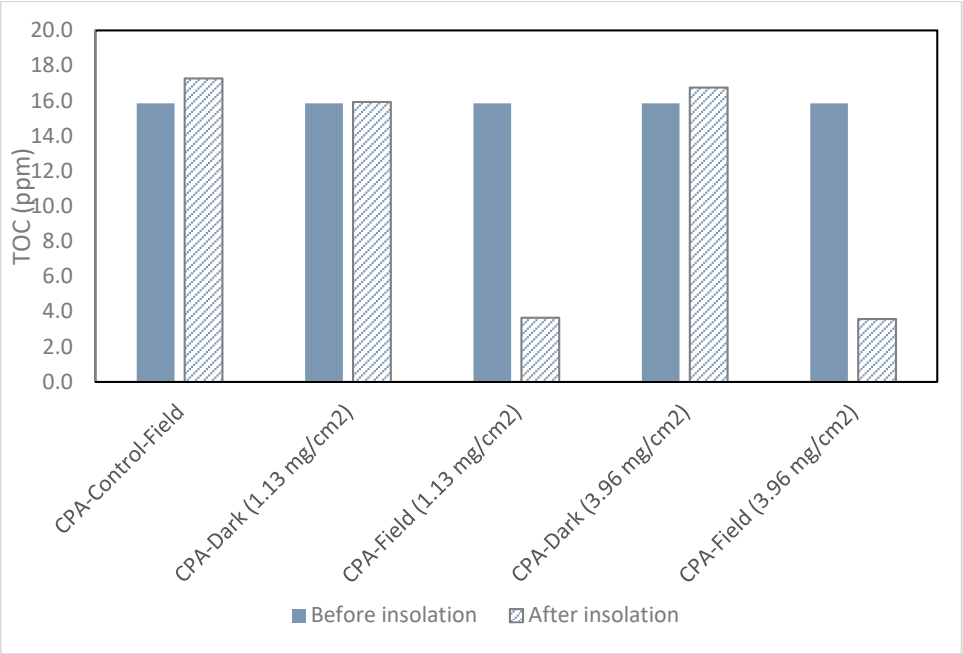


**Figure 2.** Total organic carbon (TOC) of CPA samples before and after insolation.

## 2.2. *Killex*®

Figure 3 shows the change in concentration of 2, 4-D with time, together with the cumulative energy received from sunlight during the experiments.

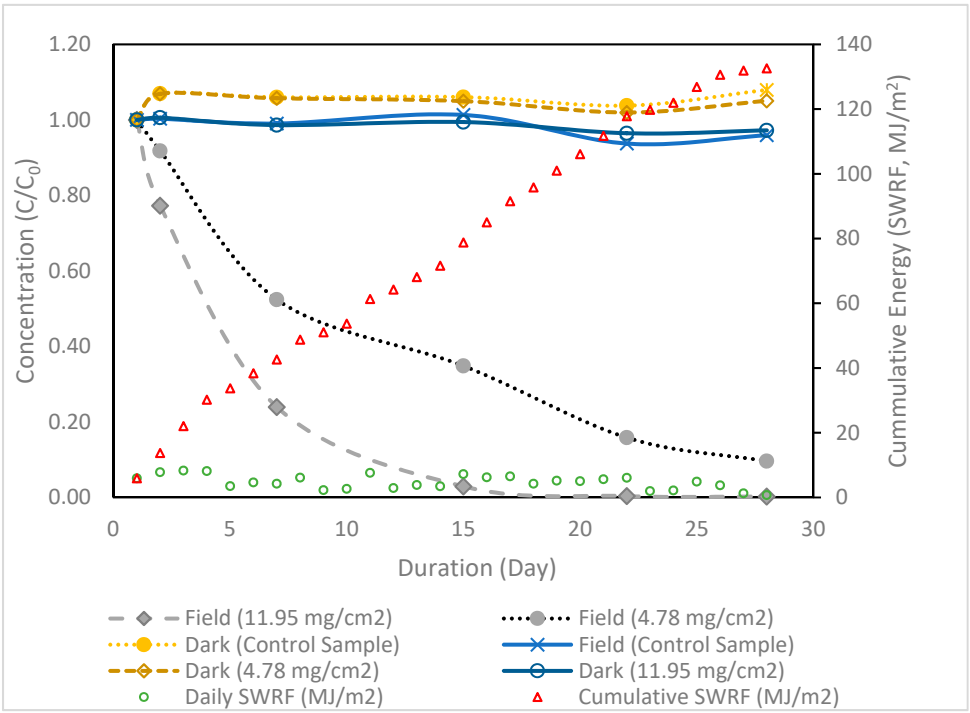


**Figure 3.** Concentration of 2, 4-D with time and energy.

At a catalyst loading of 11.95 mg/cm$^2$, 23%, 76%, and 97% of 2, 4-D was degraded after 1, 7, and 15 days, respectively. The first order kinetic rate constant (K) was 0.6 day$^{-1}$ and the total energy was 78.8 MJ/m$^2$, which is equivalent to 1.89 MJ/m$^2$ of energy from UV light. The concentration of 2, 4-D was negligible (99.8% degraded) after 22 days.

At a lower catalyst loading of 4.78 mg/cm$^2$, 8%, 48%, 65%, and 84% of 2, 4-D was degraded after 1, 7, 15, and 22 days, respectively, with a first order kinetic rate constant of K = 0.17 day$^{-1}$. The maximum degradation was 90% after 28 days of insolation and 132.61 MJ/m$^2$ energy, which is equivalent to 3.18 MJ/m$^2$ energy from UV light. The control sample under solar irradiation with no photospheres did not show any degradation. Hence it was concluded that the decrease in the concentration of 2, 4-D was the result of photocatalytic degradation in the presence of $TiO_2$ photospheres. The concentration of 2, 4-D in the indoor samples in the dark varied ±2 ppm during the study period, which confirms the effect of solar irradiation on the photocatalytic degradation process.

Figure 4 shows the concentration change of MCPP and Dicamba with time. MCPP and Dicamba were degraded entirely in 22 days at the catalyst loading of 11.95 mg/cm$^2$, whereas the concentration of MCPP and Dicamba were reduced by 94% and 74%, respectively, at the catalyst loading of 4.78 mg/cm$^2$ after 28 days. MCPP and Dicamba were not degraded in any of the control samples.

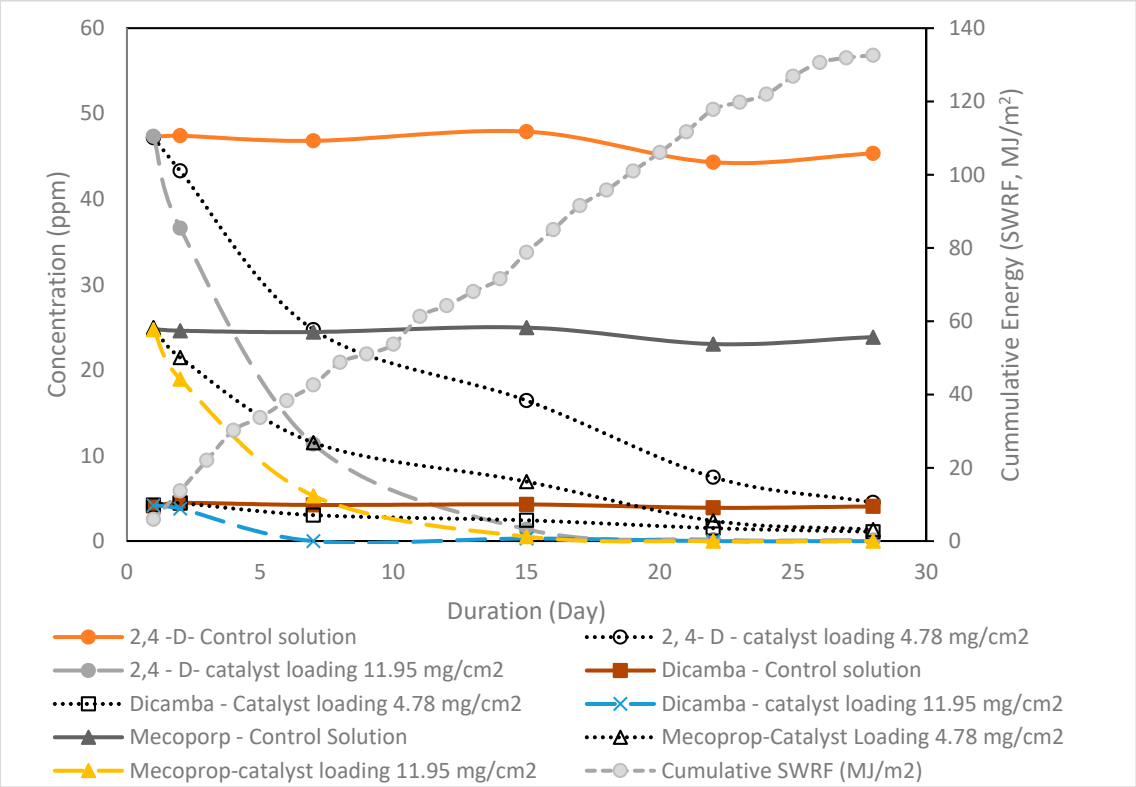


**Figure 4.** Concentration of Killex® ingredients with time and energy.

Figure 5 shows the difference between TOC of the samples before and after insolation. The TOC of the samples was reduced by 88% and 53% in the high and low catalyst loadings, respectively.

The rate of TOC removal was slower compared to the reduction in the concentration of a specific contaminant as the products of degradation were also required to be degraded. Subsequent mineralization of the degradation products led to TOC removal. Thus, TOC removal was much slower than the degradation of the parent compound.

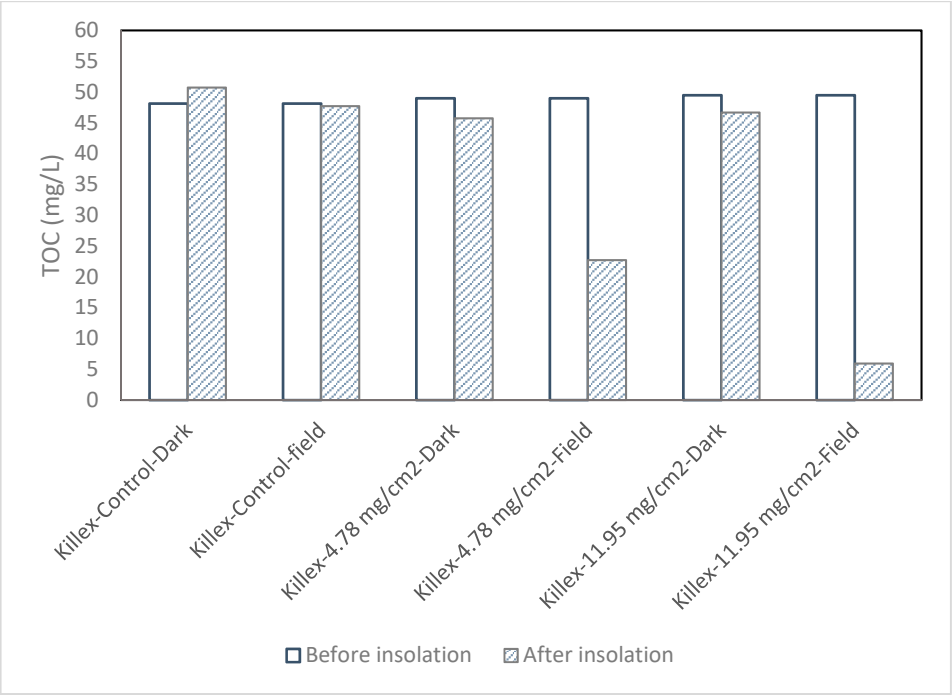


**Figure 5.** TOC of Killex® samples before and after insolation.

The results are summarized in Table 1.

**Table 1.** Summary of the Killex® experimental results.

| Catalyst Loading (mg/cm$^2$) | 11.95 | 4.78 |
|---|---|---|
| Insolation (day) | 22 | 28 |
| Degradation of 2, 4-D (%) | 99.8 | 90 |
| Degradation of Dicamba (%) | Not detectable | 74 |
| Degradation of MCPP (%) | Not detectable | 94 |
| TOC reduction in 28 days (%) | 88 | 53 |
| Kinetic rate constant (day$^{-1}$) | 0.60 | 0.17 |
| UV Energy (MJ/cm$^2$) | 1.89 | 3.18 |

Photocatalytic oxidation of 2, 4-D in the laboratory is well studied in the literature [36,75]. During degradation of 2,4-D, hydroxylation of the ring occurs followed by transformation of the aliphatic chain, as illustrated below [29]:

$$R - OCH_2 - COO^- + P^+ \rightarrow R - OCH_2^{\bullet} + CO_2$$
$$R - OCH_2^{\bullet} + O_2 \rightarrow R - OCHOO^{\bullet} + R - OCHO$$
$$R - OCH_2^{\bullet} + H^{\bullet} \rightarrow R - OCH_3$$

One of the observations during the experiments was the change in the surface characteristics of the photospheres after being exposed to solar irradiation. The photospheres were initially homogenous on the surface of water. After irradiation, an irregular distribution of the photospheres on the surface was observed and the photospheres agglomerated on the side walls of the reaction vessel. This phenomenon minimized the availability of buoyant photocatalyst spheres on the surface of the water, reducing the number of available sites on the surface of the photocatalyst to initiate the photocatalytic reaction. The higher photocatalyst loading resulted in higher degradation efficiency due to the larger available surface area for the photocatalytic reaction. However, agglomeration of photospheres was a barrier to investigating the optimum catalyst loading. Investigating an optimum surface loading of the photocatalyst should be considered for future studies on passive photocatalytic systems.

### 2.3. Sulfolane

Figure 6 shows the details of the change in the concentration of sulfolane during the experiment; 97.4% and 70.1% of sulfolane degraded at catalyst loadings of 11.95 mg/cm$^2$ and 4.78 mg/cm$^2$, respectively, during 28 days of insolation. Total energy was 132.61 MJ/m$^2$, which is equivalent to 3.18 MJ/m$^2$ energy being harvested from UV light. The first order kinetic rate constants were 0.35 day$^{-1}$ and 0.09 day$^{-1}$ at the higher and lower catalyst loadings, respectively. The control sample under solar insolation did not show any degradation; hence, the decrease in sulfolane concentration is solely a result of photocatalysis in the presence of $TiO_2$ photospheres. The final concentrations of sulfolane in the indoor samples that were kept in the dark were also reduced by 21.2% and 27.2%. The reduction in control samples in the dark could be the result of absorbance of sulfolane on the photospheres and possible biodegradation. Biodegradation of sulfolane is reported in literature [69,76]. However, the control sample without any photocatalyst in the dark showed the minimum decrease in sulfolane concentration.

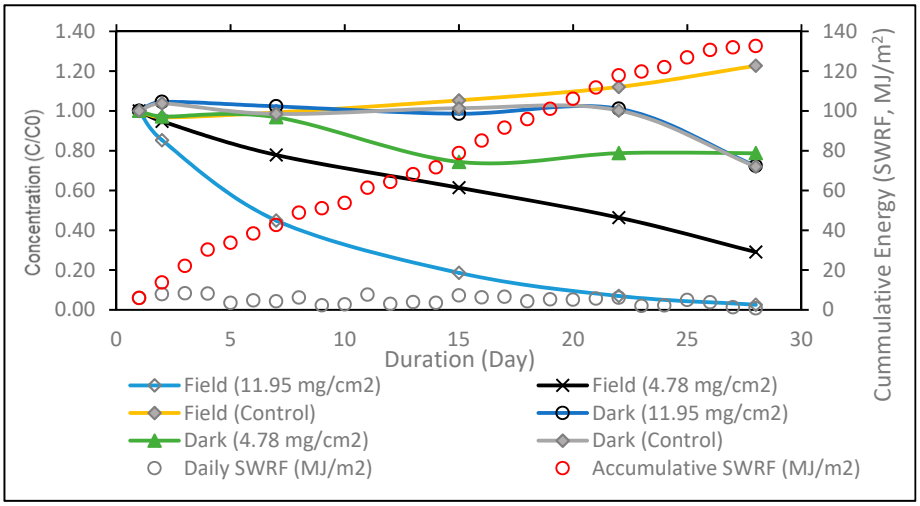


**Figure 6.** Concentration of sulfolane with time and energy.

Figure 7 shows TOC of sulfolane samples before and after solar insolation. TOC of both samples under sunlight was reduced by 64.4% and 27.75% at the catalyst loadings of 11.95 mg/cm$^2$ and 4.78 mg/cm$^2$, respectively. As can be observed, TOC reduction was not similar to the disappearance rate of sulfolane due to the contribution of its degradation products in the final TOC of the solution.

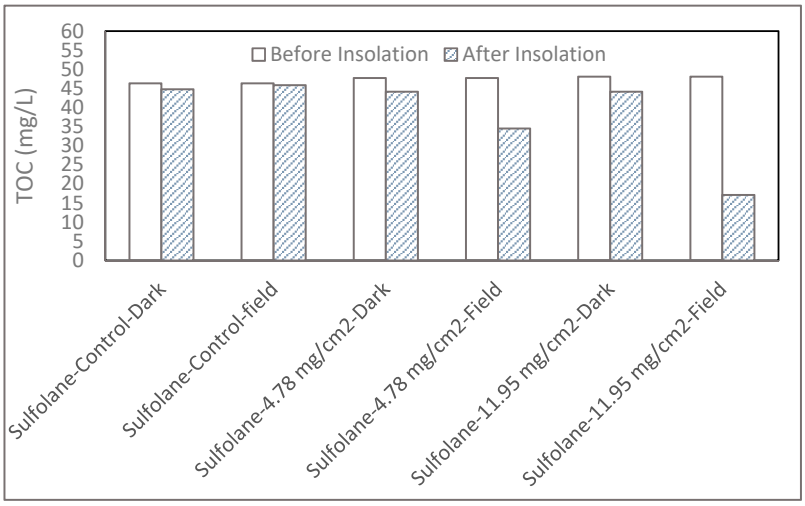


**Figure 7.** TOC of sulfolane samples before and after irradiation.

The results are summarized in Table 2.

**Table 2.** Summary of the sulfolane experimental results.

| Catalyst Loading ($mg/cm^2$) | Duration (Day) | UV Energy ($MJ/cm^2$) | Degradation of Sulfolane (%) | TOC Reduction (%) | K ($day^{-1}$) |
|---|---|---|---|---|---|
| 11.95 | 28 | 3.18 | 97.4 | 64.4 | 0.35 |
| 4.78 | | | 70.1 | 27.75 | 0.09 |

The slow rates of degradation are due to the slow mass transfer in the aqueous solution. Moreover, the amount of buoyant photocatalyst is limited to the surface area of the reaction media. Therefore, a large surface and a shallow pond are ideal for these types of reactions.

To the best of our knowledge, there are few studied on the photocatalytic oxidation of sulfolane [77–80]. The majority of these studies focused on combining a variety of oxidative methods and also photocatalysis to achieve a desired level of degradation in a photo-reactor. It was observed that under UVA irradiation, $TiO_2$ photocatalysis degraded more than 90% of sulfolane in an aqueous solution in approximately 90 min in comparison with the other advanced oxidative methods.

The findings in this research complement previous studies on the photocatalysis as a treatment option for sulfolane.

## 3. Materials

Hollow glass microspheres coated with anatase $TiO_2$ referred to as photospheres with 45 µm median diameter and density of 0.22 $g/cm^3$ were obtained from Cospheric Innovations in Microtechnology, Santa Barbara, CA, USA. BET surface area of the glass photospheres was 11.5 $m^2/g$, and they were manufactured by coating hollow glass microspheres with $TiO_2$.

Cyclopentanoic acid with purity of 99%, sulfolane with 99% purity, 99.8% pure ethyl acetate, and 99.8% pure methanol were obtained from Sigma-Aldrich (Sigma-Aldrich Canada Co.

Oakville, On, Canada). Commercially available Killex® (that containing 95 g/L of 2, 4-dichlorophenoxyacetic acid (2, 4-D), 52.5 g/L of MCPP, and 9 g/L of Dicamba) was purchased from a local retailer in Calgary, AB, Canada.

Glass jars obtained from Uline and crystallization dishes from VWR were used as reaction vessels. A Silver Line (0–2000 $mW/cm^2$) UV radiometer (M007153) (Epak Electronics Ltd., Chard, UK) was used for measuring UV intensity. A 9 $\mu V/m^2$ Eppley precision pyranometer (Model PSP) by Eppley Laboratory Inc., Newport, RI, USA was used to measure short wave radio frequency (SWRF) of solar radiation in a continuous mode.

## 4. Methods and Analysis of Samples

Initially, $TiO_2$ photospheres were floated on water, and the buoyant fraction was collected and dried overnight at room temperature. The photospheres were then mixed with water and spiked with the target contaminant using a magnetic stirrer for 30 min before irradiation. Varying concentrations of CPA, Killex®, and sulfolane were prepared by dissolving known amounts in Milli-Q water. After irradiation, samples were filtered using 0.45 um PTFE 25 mm syringe filters. The concentration of Killex® ingredients was measured using HPLC, equipped with a UV–Vis detector, and a C18 Restek Pinnacle column (Agilent Technologies Canada Inc., Mississauga, ON, Canada). The absorbance was recorded at a wavelength of 230 nm. The injection amount was 20 µL. The eluent used was water: methanol (25:75) with 10 mM phosphoric acid, and the flow rate was 1 L/min. CPA samples were analyzed using an electrospray ionization mass spectrometer (ESI–MS) (Agilent Technologies Canada Inc., Mississauga, ON, Canada). The analyte was injected using pure methanol. The capillary voltage was 4 kV, and the fragmenter voltage was 80 V.

Sulfolane was extracted from the aqueous samples with ethyl acetate. A 2 mL quantity of sample was extracted with 4 mL of ethyl acetate by vigorous shaking for 30 min [81] and analyzed by gas

chromatography equipped with a flame ionization detector (GC–FID) and a Zebron ZB-5MS column (Agilent Technologies Canada Inc., Mississauga, ON, Canada).

A Shimadzu, total organic carbon (TOC) analyzer (Shimazu, Kyoto, Japan), equipped with ASI-L auto-sampler was used to measure TOC. In all experiments, TOC was measured before and after irradiation as an indicator of mineralization.

Microsoft Excell (2013) was used for data analysis and representation (Microsoft Corporation, WA, USA).

## 5. Description of Experiments

### *5.1. Experimental Design*

All experiments were conducted at two photocatalyst loadings to evaluate the effect of surface loading and mass of the photocatalyst on degradation efficiency. In all experiments, replicate samples were monitored in the dark to evaluate the efficacy of photocatalysis and solar irradiation on the degradation, and as well to determine the adsorption of the contaminant on the catalyst surface. A control sample with no photocatalyst was used in all experiments to determine possible photolysis of the contaminant. All experiments were conducted in the field and under ambient conditions.

### *5.2. Sample Preparation*

#### 5.2.1. CPA

A 350 mL quantity of 20 ppm aqueous solution of CPA was placed in 15 cm × 7.5 cm crystallization dishes. Three samples were prepared and tested under sunlight. The control sample had no photocatalyst, and the other two contained the photocatalyst at two loading levels of 1.13 mg/cm$^2$ and 3.96 mg/cm$^2$. Experiments were conducted over a 25-day period from August to September 2016.

#### 5.2.2. Killex®

A 0.52 mL quantity of Killex® was dissolved in 1 L water, which resulted in a solution containing 49.4 ppm of 2, 4-D, 27.3 ppm of Mecoprop-p, and 4.68 ppm of Dicamba. Straight-sided glass jar containers with openings of 9 cm diameter were used as reaction vessels in the experiments. Then 250 mL of each solution was used to conduct experiments, giving a depth of 4 cm. Two levels of 4.78 mg/cm$^2$ and 11.95 mg/cm$^2$ photocatalyst loadings were tested. Volume, mass of contaminant, and depth were constant, and all the reaction vessels received a similar amount of sunlight. The experiments were conducted concurrently over a 28 day period from October to November 2016.

#### 5.2.3. Sulfolane

A 108 ppm sulfolane solution was prepared by dissolving pure sulfolane in Milli-Q water and used in the experiments. These experiments ran concurrently with the Killex® experiments described earlier. Reaction vessels, catalyst loading, and experimental conditions were identical to those of the experiment with Killex® (see Section 5.2.2).

### *5.3. Field Set-Up under Natural Sunlight and Assumptions*

Samples were protected from rainfall using a plastic cover with 20% UV absorbance. To protect wildlife and minimize their interference with the experimental setup, all samples were placed in a secured cage. To correct for evaporation, all samples were weighed and the weight was adjusted by adding Milli-Q water before sampling.

Temporal variations such as time of the day and seasonal changes control the amount of solar radiation on the Earth's surface. Further, the angle of the sun, turbidity of the atmosphere, and percentage of cloud cover impact the irradiated energy [82]. Figure 8 represents the SWRF variation during the experiments. As observed, SWRF decreased significantly from August to November 2016.

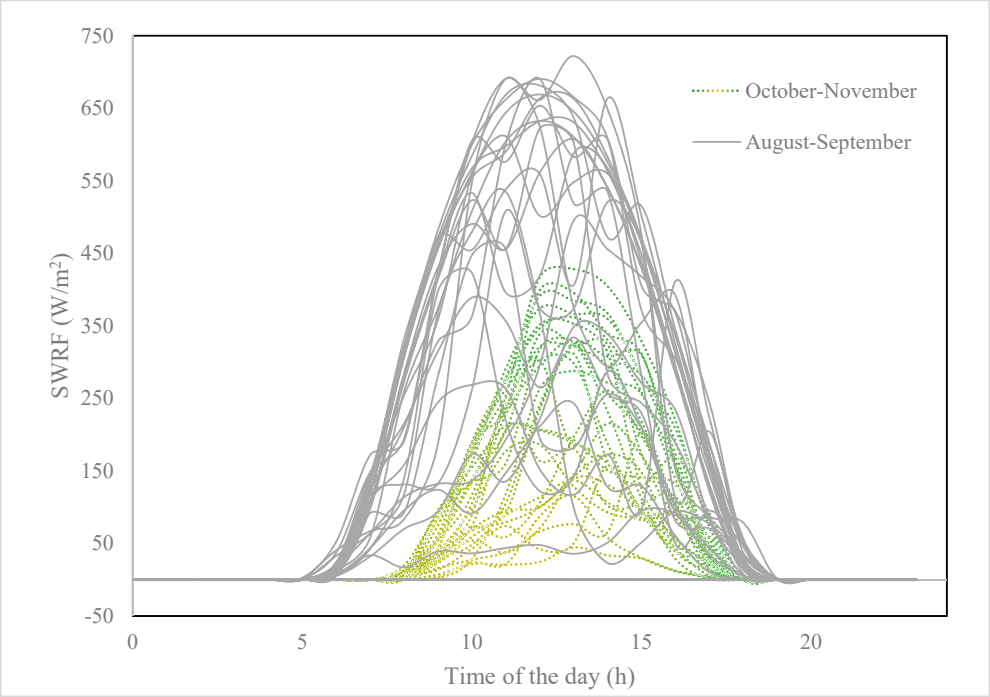


**Figure 8.** Seasonal variation of short wave radio frequency (SWRF) as a function of time of the day.

The total energy received during the experiments was calculated based on the hourly average SWRF data provided by the weather station at the University of Calgary. The data presented an average of 9.5 h daily solar light during the experiments, which was used in kinetic calculations. Based on ASTM G173-03 for the calculation of solar spectral irradiance [20] and the literature [21], it was considered that 3% of solar irradiation was composed of UV light. UV absorbance/scattering on the plastic cover was measured and it was noted that 20% of the total SWRF was absorbed/scattered by the plastic cover of the reaction vessels. Therefore, a 3% UV factor and a 20% absorbance/scattering factor were applied to all energy calculations.

## 6. Conclusions

- This research investigated the efficacy of the solar based photocatalysis in a passive mode.
- In a passive system, buoyant anatase $TiO_2$ covered hollow glass microspheres were used as a typical photocatalyst. Killex®, CPA and sulfolane were selected as the model contaminants.
- In the Killex® solution, Dicamba and MCPP were completely degraded, 2, 4-D was degraded up to 99.8%, and sulfolane and CPA were also degraded by 97.4% and 100% in aqueous solutions, respectively.
- TOC of Killex® samples were reduced by 53% and 88% with catalyst loadings of 4.78 mg/cm$^2$ and 11.95 mg/cm$^2$, respectively. The same trend was observed in sulfolane samples, where TOC decreased by 28% and 64% at catalyst loadings of 4.78 mg/cm$^2$ and 11.95 mg/cm$^2$, respectively. TOC in CPA solutions also decreased by approximately 77% at the both catalyst loadings.
- The results confirmed the effectiveness of the passive photocatalysis under natural sunlight in the northern climate (latitude: 51°, 4′ N, longitude: 114°, 8′ W; altitude: 1114 m) using buoyant photospheres, and during the late summer and fall season.
- This study established what should be expected of a passive photocatalysis system in terms of duration and reaction rates in the ambient environment.
- The findings confirmed the efficacy of the passive system in the selected geographical region. However, there are limitations for using a buoyant powdered photocatalyst in the ambient environment including collection after treatment, digestion by wildlife, and spreading in the

unwanted streams. These limitations necessitate the additional research for development of a more easily deployable photocatalyst for such applications.

**Author Contributions:** G.H. designed the study, performed the literature review, conducted the experiments, analyzed the results, and wrote the initial draft of the paper. C.H.L. oversaw the research and supported the experimental design and field set-up. G.A. supervised the research and supported experimental design, conducted data analysis, and reviewed the final paper.

**Funding:** This research was partially funded by CMC Research Institutes, MITACS, and the Natural Sciences and Engineering Research Council of Canada (NSERC).

**Acknowledgments:** The authors acknowledge the partial financial assistance provided by the Natural Science and Engineering Research Council of Canada, Mitacs, and CMC Research Institutes. The authors would also thank the Department of Geography of the University of Calgary for providing access to the weather research station and supplying weather data during this research.

**Conflicts of Interest:** The authors declare no conflict of interest.

## References

1. Khetarpal, D.; Yassaa, N.; Nzotcha, U.; Asthana, A.; Kasture, M.; Bizzarri, F. *World Energy Resources: Solar 2016*; World Energy Council: London, UK, 2016.
2. Blanco, E.; González-Leal, J.M.; Ramírez-del Solar, M. Photocatalytic $TiO_2$ sol–gel thin films: Optical and morphological characterization. *Sol. Energy* **2015**, *122*, 11–23. [CrossRef]
3. International Energy Agency. *Key World Energy Statistics*; International Energy Agency: Paris, France, 2017.
4. Farrauto, R.J.; Heck, R.M. Environmental catalysis into the 21st century. *Catal. Today* **2000**, *55*, 179–187. [CrossRef]
5. Gazea, B.; Adam, K.; Kontopoulos, A. A review of passive systems for the treatment of acid mine drainage. *Miner. Eng.* **1996**, *9*, 23–42. [CrossRef]
6. Mostafa, S. Sunlight-Induced Photochemical Processes in Natural and Wastewater Treatment Systems. Ph.D. Thesis, University of Colorado, Boulder, CO, USA, 2015.
7. Mekhilef, S.; Saidur, R.; Safari, A. A review on solar energy use in industries. *Renew. Sustain. Energy Rev.* **2011**, *15*, 1777–1790. [CrossRef]
8. Bradford, T. *Solar Revolution: The Economic Transformation of the Global Energy Industry*; MIT Press: Cambridge, MA, USA, 2008; ISBN 9780262269094.
9. Blanco, J.; Malato, S.; Fernández-Ibañez, P.; Alarcón, D.; Gernjak, W.; Maldonado, M.I. Review of feasible solar energy applications to water processes. *Renew. Sustain. Energy Rev.* **2009**, *13*, 1437–1445. [CrossRef]
10. Danwittayakul, S.; Jaisai, M.; Dutta, J. Efficient solar photocatalytic degradation of textile wastewater using ZnO/ZTO composites. *Appl. Catal. B Environ.* **2015**, *163*, 1–8. [CrossRef]
11. Spasiano, D.; Marotta, R.; Malato, S.; Fernandez-Ibañez, P.; Di Somma, I. Solar photocatalysis: Materials, reactors, some commercial, and pre-industrialized applications. A comprehensive approach. *Appl. Catal. B Environ.* **2015**, *170–171*, 90–123. [CrossRef]
12. Yu, L.; Achari, G.; Langford, C.H. LED-based photocatalytic treatment of pesticides and chlorophenols. *J. Environ. Eng.* **2013**, *139*, 1146–1151. [CrossRef]
13. Wold, A. Photocatalytic properties of $TiO_2$. *Chem. Mater.* **1993**, *5*, 280–283. [CrossRef]
14. Akolekar, D.B.; Bhargava, S.K.; Shirgoankar, I.; Prasad, J. Catalytic wet oxidation: An environmental solution for organic pollutant removal from paper and pulp industrial waste liquor. *Appl. Catal. A Gen.* **2002**, *236*, 255–262. [CrossRef]
15. Ghosh, J.P.; Langford, C.H.; Achari, G. Characterization of an LED based photoreactor to degrade 4-chlorophenol in an aqueous medium using coumarin (C-343) sensitized $TiO_2$. *J. Phys. Chem. A* **2008**, *112*, 10310–10314. [CrossRef] [PubMed]
16. Allen, N.S.; Edge, M.; Verran, J.; Stratton, J.; Maltby, J.; Bygott, C. Photocatalytic titania based surfaces: Environmental benefits. *Polym. Degrad. Stab.* **2008**, *93*, 1632–1646. [CrossRef]
17. Fujishima, A.; Zhang, X.; Tryk, D. $TiO_2$ photocatalysis and related surface phenomena. *Surf. Sci. Rep.* **2008**, *63*, 515–582. [CrossRef]
18. Blake, D.M. Bibliography of work on the heterogeneous photocatalytic removal of hazardous compounds from water and air. *Natl. Renew. Energy Lab.* **2001**, *4*, 1–265. [CrossRef]

19. Akpan, U.G.; Hameed, B.H. Parameters affecting the photocatalytic degradation of dyes using $TiO_2$-based photocatalysts: A review. *J. Hazard. Mater.* **2009**, *170*, 520–529. [CrossRef] [PubMed]
20. ASTM International. *Standard Tables for Reference Solar Spectral Irradiances: DIRECT, Normal and Hemispherical on 37° Tilted Surface*; Standard G173-03; ASTM International: West Conshohocken, PA, USA, 2013; ISBN G 173 03.
21. Langford, C.H. Photocatalysis—A special issue on a unique hybrid rea of catalysis. *Catalysts* **2012**, *2*, 327–329. [CrossRef]
22. Keane, D.A.; McGuigan, K.G.; Ibáñez, P.F.; Polo-López, M.I.; Byrne, J.A.; Dunlop, P.S.M.; O'Shea, K.; Dionysiou, D.D.; Pillai, S.C. Solar photocatalysis for water disinfection: Materials and reactor design. *Catal. Sci. Technol.* **2014**, *4*, 1211–1226. [CrossRef]
23. Zahedi, F.; Behpour, M.; Ghoreishi, S.M.; Khalilian, H. Photocatalytic degradation of paraquat herbicide in the presence $TiO_2$ nanostructure thin films under visible and sun light irradiation using continuous flow photoreactor. *Sol. Energy* **2015**, *120*, 287–295. [CrossRef]
24. Chen, X.; Mao, S.S. Titanium dioxide nanomaterials: Synthesis, properties, modifications and applications. *Chem. Rev.* **2007**, *107*, 2891–2959. [CrossRef]
25. Portjanskaja, E.; Krichevskaya, M.; Preis, S.; Kallas, J. Photocatalytic oxidation of humic substances with $TiO_2$-coated glass micro-spheres. *Environ. Chem. Lett.* **2004**, *2*, 123–127. [CrossRef]
26. Sakthivel, S.; Shankar, M.V.; Palanichamy, M.; Arabindoo, B.; Murugesan, V. Photocatalytic decomposition of leather dye comparative study of $TiO_2$ supported on alumina and glass beads. *J. Photochem. Photobiol. A Chem.* **2002**, *148*, 153–159. [CrossRef]
27. Miranda-García, N.; Suárez, S.; Sánchez, B.; Coronado, J.M.; Malato, S.; Maldonado, M.I. Photocatalytic degradation of emerging contaminants in municipal wastewater treatment plant effluents using immobilized $TiO_2$ in a solar pilot plant. *Appl. Catal. B Environ.* **2011**, *103*, 294–301. [CrossRef]
28. Sirisuk, A.; Hill, C.G.; Anderson, M.A. Photocatalytic degradation of ethylene over thin films of titania supported on glass rings. *Catal. Today* **1999**, *54*, 159–164. [CrossRef]
29. Guillard, C.; Amalric, L.; D'Oliveira, J.C.; Delpart, H.; Hoang-Van, C.; Pichat, P. Heterogeneous photocatalysis: Use in water treatment and involvement in atmopheric chemistry. In *Aquatic and Surface Photochemistry*; Helz, G.R., Zepp, R.G., Crosby, D.G., Eds.; Lewis Publishers: Boca Raton, FL, USA, 1994; pp. 369–386. ISBN 0-87371-871-2.
30. Malato, S.; Fernández-Ibáñez, P.; Maldonado, M.I.; Blanco, J.; Gernjak, W. Decontamination and disinfection of water by solar photocatalysis: Recent overview and trends. *Catal. Today* **2009**, *147*, 1–59. [CrossRef]
31. Chekir, N.; Boukendakdji, H.; Igoud, S.; Taane, W. Solar energy for the benefit of water treatment: Solar photoreactor. *Procedia Eng.* **2012**, *33*, 174–180. [CrossRef]
32. Abdel-Maksoud, Y.; Imam, E.; Ramadan, A. $TiO_2$ solar photocatalytic reactor systems: Selection of reactor design for scale-up and commercialization—Analytical review. *Catalysts* **2016**, *6*, 138. [CrossRef]
33. Goswami, D.Y. *Principles of Solar Engineering*, 3rd ed.; CRC Press: Boca Raton, FL, USA; Taylor and Francis Group: Abingdon, UK, 2015; Volume 1, ISBN 1466563796.
34. Goswami, D.Y.; Kreith, F.; Kreider, J.F. *Principles of Solar Engineering*, 2nd ed.; Taylor & Francis Group: Philadelphia, PA, USA, 2000.
35. Feitz, A.J.; Boyden, B.H.; Waite, T.D. Evaluation of two solar pilot scale fixed-bed photocatalytic reactors. *Water Res.* **2000**, *34*, 3927–3932. [CrossRef]
36. Toor, A.P.; Verma, A.; Jotshi, C.K.; Bajpai, P.K.; Singh, V. Photocatalytic degradation of 3, 4-dichlorophenol using $TiO_2$ in a shallow pond slurry reactor. *Indian J. Chem. Technol.* **2005**, *12*, 75–81.
37. Heller, A.; Brock, J. Materials and Methods for Photocatalyzing Oxidation of Organic Compounds on Water. U.S. Patent 4,997,576, 25 September 1989.
38. Yuan, J.; An, Z.-G.; Zhang, J.-J.; Li, B. Synthesis and properties of hollow glass spheres/$TiO_2$ composite. *Imaging Sci. Photochem.* **2012**, *30*, 447–455.
39. Wang, J.; He, B.; Kong, X.Z. A study on the preparation of floating photocatalyst supported by hollow $TiO_2$ and its performance. *Appl. Surf. Sci.* **2015**, *327*, 406–412. [CrossRef]
40. Maki, Y.; Ide, Y.; Okada, T. Water-floatable organosilica particles for $TiO_2$ photocatalysis. *Chem. Eng. J.* **2016**, *299*, 367–372. [CrossRef]
41. Shifu, C.; Gengyu, C. Photocatalytic degradation of organophosphorus pesticides using floating photocatalyst $TiO_2$ • $SiO_2$/beads by sunlight. *Sol. Energy* **2005**, *79*, 1–9. [CrossRef]

42. Shifu, C.; Gengyu, C. Photocatalytic oxidation of nitrite by sunlight using $TiO_2$ supported on hollow glass microbeads. *Sol. Energy* **2002**, *73*, 15–21. [CrossRef]
43. Hartley, A.C.; Moss, J.B.; Keesling, K.J.; Moore, N.J.; Glover, J.D.; Boyd, J.E. PMMA-titania floating macrospheres for the photocatalytic remediation of agro-pharmaceutical wastewater. *Water Sci. Technol.* **2017**, *75*, 1362–1369. [CrossRef] [PubMed]
44. Xing, Z.; Zhang, J.; Cui, J.; Yin, J.; Zhao, T.; Kuang, J.; Xiu, Z.; Wan, N.; Zhou, W. Recent advances in floating $TiO_2$-based photocatalysts for environmental application. *Appl. Catal. B Environ.* **2018**, *225*, 452–467. [CrossRef]
45. Preis, S.; Krichevskaya, M.; Kharchenko, A. Photocatalytic oxidation of aromamtic aminocompounds in aqueous solutions and groundwater from abandoned military bases. *Water Sci. Technol.* **1997**, *35*, 265–272. [CrossRef]
46. Welch, K. Passive purification-effectiveness of photocatalytic titanium dioxide to convert pathogens and pollutants. *Am. Ceram. Soc. Bull.* **2014**, *93*, 25–30.
47. Komtchou, S.; Dirany, A.; Drogui, P. Traitement des eaux contaminées par les pesticides—Pour le treatment des eaux contaminees par les pesticides-revue de litterature. *Rev. Sci. l'eau* **2018**, *29*, 231–262. [CrossRef]
48. Hashimoto, K.; Irie, H.; Fujishima, A. A historical overview and future prospects. *Jpn. J. Appl. Phys.* **2005**, *44*, 8269–8285. [CrossRef]
49. Magalhães, F.; Lago, R.M. Floating photocatalysts based on $TiO_2$ grafted on expanded polystyrene beads for the solar degradation of dyes. *Sol. Energy* **2009**, *83*, 1521–1526. [CrossRef]
50. Magalhães, F.; Moura, F.C.C.; Lago, R.M. $TiO_2$/LDPE composites: A new floating photocatalyst for solar degradation of organic contaminants. *Desalination* **2011**, *276*, 266–271. [CrossRef]
51. Sboui, M.; Faouzi, M.; Rayes, A.; Ochiai, T.; Houas, A. Application of solar light for photocatalytic degradation of Congo red by a floating salicylic acid-modified $TiO_2$/palm trunk photocatalyst. *Comptes Rendus Chim.* **2017**, *20*, 181–189. [CrossRef]
52. Leshuk, T.; Krishnakumar, H.; de Oliveira Livera, D.; Gu, F. Floating photocatalysts for passive solar degradation of naphthenic acids in oil sands process-affected water. *Water* **2018**, *10*, 202. [CrossRef]
53. Robert, D.; Keller, V.; Keller, N. Immobilization of a semi-conductor photocatalyst on solid supports, methods, materials and applications. In *Photocatalysis and Water Purification: From Fundamentals to Recent Applications*; Lu, M., Pichat, P., Eds.; Wiley-VCH: Weinheim, Germany, 2013; pp. 145–172. ISBN 9783527645411.
54. Gong, X.-Q.; Selloni, A. Reactivity of Anatase $TiO_2$ Nanoparticles: The Role of the Minority (001) Surface. *J. Phys. Chem. B* **2005**, *109*, 19560–19562. [CrossRef]
55. Nakamura, R.; Ohashi, N.; Imanishi, A.; Osawa, T.; Matsumoto, Y.; Koinuma, H.; Nakato, Y. Crystal-Face Dependences of Surface Band Edges and Hole Reactivity, Revealed by Preparation of Essentially Atomically Smooth and Stable (110) and (100) n-$TiO_2$ (Rutile) Surfaces. *J. Phys. Chem. B* **2005**, *109*, 1648–1651. [CrossRef]
56. Ong, W.-J.; Tan, L.-L.; Chai, S.-P.; Yong, S.-T.; Mohamed, A.R. Highly reactive {001} facets of $TiO_2$-based composites: Synthesis formation mechanism and characterization. *Nanoscale* **2014**, *6*, 1946–2008. [CrossRef]
57. Tian, T.; Hu, J.; Xiao, Z. Research Advances in Photocatalysis of Inorganic Hollow Spheres. *World J. Nano Sci. Eng.* **2014**, *4*, 111–125. [CrossRef]
58. Zeng, Y.; Wang, X.; Wang, H.; Dong, Y.; Ma, Y.; Yao, J. Multi-shelled titania hollow spheres fabricated by a hard template strategy: Enhanced photocatalytic activity. *Chem. Commun.* **2010**, *46*, 4312–4314. [CrossRef]
59. Li, S.; Chen, J.; Zheng, F.; Li, Y.; Huang, F. Synthesis of the double-shell anatase–rutile $TiO_2$ hollow spheres with enhanced photocatalytic activity. *Nanoscale* **2013**, *5*, 12150–12155. [CrossRef]
60. Tao, Y.; Xu, Y.; Pan, J.; Gu, H.; Qin, C.; Zhou, P. Glycine assisted synthesis of flower-like $TiO_2$ hierarchical spheres and its application in photocatalysis. *Mater. Sci. Eng. B* **2012**, *177*, 1664–1671. [CrossRef]
61. Natural Resources Canada Oil Sands: Water Management, a Strategic Resource for Canada, North America and the Global Market. Available online: https://www.nrcan.gc.ca/energy/publications/18750 (accessed on 8 February 2017).
62. Province of Alberta. *Environmental Protection and Enhancement Act, Revised Statutes of Alberta 2000*; Chapter E-12; Alberta Queen's Printer: Edmonton, AB, Canada, 2000; pp. 1–164.
63. Kannel, P.R.; Gan, T.Y. Naphthenic acids degradation and toxicity mitigation in tailings wastewater systems and aquatic environments: A review. *J. Environ. Sci. Health Part A Tox. Hazard. Subst. Environ. Eng.* **2012**, *47*, 1–21. [CrossRef] [PubMed]

64. Grewer, D.M.; Young, R.F.; Whittal, R.M.; Fedorak, P.M. Naphthenic acids and other acid-extractables in water samples from Alberta: What is being measured? *Sci. Total Environ.* **2010**, *408*, 5997–6010. [CrossRef] [PubMed]
65. Leshuk, T.; Wong, T.; Linley, S.; Peru, K.M.; Headley, J.V.; Gu, F. Solar photocatalytic degradation of naphthenic acids in oil sands process-affected water. *Chemosphere* **2016**, *144*, 1854–1861. [CrossRef] [PubMed]
66. Health Canada Special Review of 2,4-D: Proposed Decision for Consultation. Available online: https://www.canada.ca/en/health-canada/services/consumer-product-safety/pesticides-pest-management/public/consultations/re-evaluation-note/2016/special-review-2-4-d/document.html#s2 (accessed on 8 February 2017).
67. Krieger, R. *Hayes' Handbook of Pesticide Toxicology*; Krieger, R., Ed.; Elsevier Science & Technology: Saint Louis, MS, USA, 2010; ISBN 9780080922010.
68. Giri, R.R.; Ozaki, H.; Taniguchi, S.; Takanami, R. Photocatalytic ozonation of 2,4-dichlorophenoxyacetic acid in water with a new $TiO_2$ fiber. *Int. J. Environ. Sci. Technol.* **2008**, *5*, 17–26. [CrossRef]
69. Ikehata, K.; El-Din, M.G.; Snyder, S.A. Ozonation and advanced oxidation treatment of emerging organic pollutants in water and wastewater. *Ozone Sci. Eng.* **2008**, *30*, 21–26. [CrossRef]
70. Anderson, A.; Byrtus, G.; Thompson, J.; Humphries, D.; Hill, B.; Bilyk, M.; Alberta. Dept. of Environment. Water Research User Group. *Baseline Pesticide Data for Semi-Permanent Wetlands in the Aspen Parkland of Alberta*; Alberta Environment: Edmonton, Alberta, 2002.
71. Canadian Council of Ministers of Envivronment. *Canadian Soil Quality Guidelines for the Protection of Environmental and Human Health—Sulfolane*; Canadian Council of Ministers of the Environment: Winnipeg, MB, Canada, 2006.
72. Leigh, M.B.; Barnes, D. Water and Environmental Research Center, annual technical report. In *Toxicity of Sulfolane Breakdown Products in Contaminated Groundwater*; Water and Environmental Research Center: University of Alaska Fairbanks, AK, USA, 2013.
73. Greene, E.A.; Beatty, P.H.; Fedorak, P.M. Sulfolane degradation by mixed cultures, and a bacterial isolate identified as a Variovorax sp. *Arch. Microbiol.* **2000**, *174*, 111–119. [CrossRef]
74. Suh, S.; Tomar, S.; Leighton, M.; Kneifel, J. Environmental performance of green building code and certification systems. *Environ. Sci. Technol.* **2014**, *48*, 2551–2560. [CrossRef]
75. Lee, S.C.; Hasan, N.; Lintang, H.O.; Shamsuddin, M.; Yuliati, L. Photocatalytic removal of 2,4-dichlorophenoxyacetic acid herbicide on copper oxide/titanium dioxide prepared by co-precipitation method. *IOP Conf. Ser. Mater. Sci. Eng.* **2016**, *107*. [CrossRef]
76. Yang, Y.; Yu, L.; Achari, G. Case Study: Evaluation of Pure and Mixed Bacterial Cultures on Sulfolane Biodegradation in Aqueous Media. In Proceedings of the CSCE Annual Conference, Montreal, QC, Canada, 12–15 June 2019.
77. Yu, L.; Mehrabani-Zeinabad, M.; Achari, G.; Langford, C. Application of UV based advanced oxidation to treat sulfolane in an aqueous medium. *Chemosphere* **2016**, *160*, 155–161. [CrossRef]
78. Izadifard, M. Oxidation of Sulfolane in Aqueous Systems by Chemical and Photochemical Processes. Ph.D. Thesis, University of Calgary, Calgary, AB, Canada, 2019.
79. Brandão, M.; Yu, L.; Garcia, C.; Achari, G. Advanced oxidation based treatment of soil wash water contaminated with sulfolane. *Water* **2019**, *11*, 2152. [CrossRef]
80. Mehrabani-Zeinabad, M. Advanced Oxidative Processes for Treatment of Emerging Contaminants in Water. Ph.D. Thesis, University of Calgary, Calgary, AB, Canada, 2016.
81. Versace, F.; Uppugunduri, C.R.S.; Krajinovic, M.; The, Y.; Gumy, F.P.; Mangin, P.; Staub, C.; Ansari, M. A novel method for quantification of sulfolane (a metabolite of busulfan) in plasma by gas chromatography-tandem mass spectrometry. *Anal. Bioanal. Chem.* **2012**, *404*, 1831–1838. [CrossRef] [PubMed]
82. Sen, Z. *Solar Energy Fundamentals and Modeling Techniques*; Springer-Verlag: London, UK, 2008; ISBN 9781848001336.